

Modeling Pc4 Pulsations in Two and a Half Dimensions

DRAFT VERSION CREATED ON FEBRUARY 6, 2016

© Charles A McEachern 2016
ALL RIGHTS RESERVED

Acknowledgements

Acknowledgement placeholder.

Dedication

Dedication placeholder.

Abstract

Abstract placeholder.

Contents

Acknowledgements	i
Dedication	ii
Abstract	iii
List of Tables	vii
List of Figures	viii
1 The Near-Earth Environment	1
1.1 The Outer Magnetosphere	2
1.1.1 The Magnetopause	2
1.1.2 The Magnetotail	2
1.1.3 Cusp Regions	2
1.2 The Inner Magnetosphere	2
1.2.1 The Plasmasphere	3
1.2.2 Ring Currents	3
1.2.3 The Radiation Belts	3
1.3 Geomagnetic Disturbances	3
1.3.1 Storms	3
1.3.2 Substorms	3
2 Pc4 Pulsations	4
2.1 Observations	4

2.2	Theoretical Work	5
2.3	Giant Pulsations	5
3	Waves in Cold Resistive Plasmas	6
3.1	Parallel Propagation Limit	7
3.1.1	Parallel Polarization	8
3.1.2	Perpendicular Polarization	8
3.2	Perpendicular Propagation Limit	9
3.2.1	Parallel Polarization	9
3.2.2	Perpendicular Polarization	10
3.3	High Altitude Limit	10
3.3.1	Azimuthal Polarization	11
3.3.2	Meridional Polarization	11
3.4	Implications for This Work	11
3.4.1	Mode Coupling	11
3.4.2	High Modenumber Cutoff	12
4	Numerical Model	13
4.1	Coordinate System	14
4.1.1	Covariant and Contravariant Bases	16
4.1.2	Mapping to Physical Coordinates	17
4.2	Ionospheric Profile	18
4.2.1	Conductivity	18
4.2.2	Alfvén Speed	19
4.3	Maxwell’s Equations	20
4.3.1	Notation and Optimization	20
4.3.2	Magnetic Fields	21
4.3.3	Electric Fields	22
4.4	Driving	24
4.4.1	Outer Boundary Compression	25
4.4.2	Ring Current Modulation	25
4.5	Boundary Conditions	27
4.5.1	Parity and Interpolation	27

4.5.2	Coupling to the Atmosphere	28
5	Electron Inertial Effects	30
5.1	The Boris Approximation	34
5.2	Field-Aligned Currents	34
5.3	Inertial Length Scales	34
6	Large Modenumber Effects	35
6.1	Finite Poloidal Lifetimes	35
6.2	Development of Fine Structure	36
6.3	Damping of Ground Signatures	36
6.4	Electromagnetic Energy Gap	36
7	Evolution of Giant Pulsations	37
8	Comparison to Van Allen Probe Observations	38
9	Conclusion and Discussion	39
9.1	Future Work	39
	References	40
	Appendix A. Differential Geometry	42
A.1	Glossary	42
A.2	Acronyms	42
	Appendix B. Integrating Factors	43

List of Tables

A.1	Acronyms	42
-----	--------------------	----

List of Figures

4.1 Ionospheric Conductivity Profiles	19
---	----

Chapter 1

The Near-Earth Environment

It's all about energy transfer!

Some example citations, including a few with special characters: [1], [2], [3].

Sun generates energy through nuclear reactions.

This energy drives behavior in the near-Earth environment.

Typical solar wind density is $\sim 5/\text{cm}^3$. Typical solar wind velocity at Earth is 10^2 km/s to 10^3 km/s . Typical solar wind particle energy is 1 keV to 10 keV. Density can vary by ~ 3 orders of magnitude, and velocity by one, during times of high solar activity. CMEs can also mess with the north/south component of the interplanetary magnetic field.

45° angle with the Earth-Sun line, which is the X direction.¹

Solar wind is what deforms Earth's magnetic field to form the magnetosphere.

Transient solar wind phenomena, such as coronal mass ejections, are also known to be related to geomagnetic disturbances at Earth. Jesse cites here:

R. L. McPherron. Physical processes producing magnetospheric substorms and magnetic

¹We use uppercase X , Y , and Z to indicate GSE coordinates: X points from the Earth to the Sun. Y is perpendicular to X , and in the Sun's ecliptic plane, pointing duskwards... against Earth's orbital motion. Points north, out of the ecliptic plane. Later, we will use lowercase x , y , and z to define a more-or-less analogous coordinate system with respect to Earth.

storms. In J. A. Jacobs, editor, Geomagnetism, volume 4, chapter 7. Academic Press, 1991.

G. Rostoker. Substorms. In Handbook of the Solar-Terrestrial Environment, chapter 15. Springer-Verlag, 2007.

This might just be worth tracking down... Jesse cites several chapters:

M. Shulz. Magnetospheres. In Handbook of the Solar-Terrestrial Environment, chapter 7. Springer-Verlag, 2007.

1.1 The Outer Magnetosphere

The outer magnetosphere is a region where the field lines are closed, but significantly deformed by the solar wind.

1.1.1 The Magnetopause

1.1.2 The Magnetotail

1.1.3 Cusp Regions

1.2 The Inner Magnetosphere

In the inner magnetosphere, field lines are closed, and are approximately dipolar.

1.2.1 The Plasmasphere

1.2.2 Ring Currents

1.2.3 The Radiation Belts

1.3 Geomagnetic Disturbances

1.3.1 Storms

1.3.2 Substorms

Chapter 2

Pc4 Pulsations

TODO: Fujita and Tamao 1988, Greifinger and Greifinger 1968, 1973 showed that the poloidal and toroidal modes act differently at the ionosphere.

TODO: Hughes 1974: Hall conducting ionosphere reflects ULF wave fields. Well-known result.

TODO: Theoretical consideration of decay vs propagation, by frequency. Lysak and Yoshikawa 2006.

TODO: Takahashi 2013 saw a high-modenumber poloidal mode with THEMIS.

TODO: Fishbone instability. McGuire 1983, Chen 1984. Similar phenomenon, but for lab plasmas.

2.1 Observations

Dai noted specifically that it was unclear why poloidal Pc4 pulsations were preferentially seen on the dayside, since drift resonance should be azimuthally distributed.

2.2 Theoretical Work

2.3 Giant Pulsations

Chapter 3

Waves in Cold Resistive Plasmas

Cold, linearized Ampère's Law and Faraday's Law. The vector \underline{B} is the perturbation to the zeroth-order magnetic field.

$$\frac{\partial}{\partial t} \underline{B} = -\nabla \times \underline{E} \qquad \underline{\epsilon} \cdot \frac{\partial}{\partial t} \underline{E} = \frac{1}{\mu_0} \nabla \times \underline{B} - \underline{J} \quad (3.1)$$

Ohm's Law. Electron inertial effects are included in the parallel direction. See chapter 5.

$$\frac{m_e}{ne^2} \frac{\partial}{\partial t} J_{\parallel} = \sigma_0 E_{\parallel} - J_{\parallel} \qquad 0 = \underline{\sigma}_{\perp} \cdot \underline{E}_{\perp} - \underline{J}_{\perp} \quad (3.2)$$

Suppose that the fields and currents are resonating as $\exp(i\underline{k} \cdot \underline{x} - i\omega t)$. Evaluate the derivatives. Eliminate magnetic fields and currents.

$$0 = E_{\parallel} + \frac{c^2}{\omega^2} (\underline{k} \underline{k} \cdot \underline{E} - k^2 \underline{E})_{\parallel} + \frac{i\omega_P^2}{\omega(\nu - i\omega)} E_{\parallel} \quad (3.3)$$

$$0 = \underline{E}_{\perp} + \frac{v_A^2}{\omega^2} (\underline{k} \underline{k} \cdot \underline{E} - k^2 \underline{E})_{\perp} + \frac{i}{\epsilon_{\perp} \omega} \underline{\sigma}_{\perp} \cdot \underline{E}_{\perp} \quad (3.4)$$

The above expression makes use of the vector identity $\underline{k} \times \underline{k} \times \underline{E} = \underline{k} \underline{k} \cdot \underline{E} - k^2 \underline{E}$. The Alfvén speed, speed of light, plasma frequency, and parallel conductivity are defined in

the usual way:

$$v_A^2 \equiv \frac{1}{\mu_0 \epsilon_\perp} \quad c^2 \equiv \frac{1}{\mu_0 \epsilon_0} \quad \omega_P^2 \equiv \frac{ne^2}{m_e \epsilon_0} \quad \sigma_0 \equiv \frac{ne^2}{m_e \nu} \quad (3.5)$$

Note that this definition of the Alfvén speed takes into account the displacement current correction which is important when v_A approaches c .

Without loss of generality, the wave vector \underline{k} can be said to lie in the x - z plane; the distinction between the x and y directions is revisited in section 3.4. Let θ be the angle between \underline{k} and the zeroth-order magnetic field.

Then equations (3.3) and (3.4) can be combined into the usual dispersion tensor form, $\underline{\underline{T}} \cdot \underline{E} = 0$, where

$$\underline{\underline{T}} = \underline{\underline{\mathbb{I}}} + \frac{k^2}{\omega^2} \begin{bmatrix} -v_A^2 \cos^2 \theta & 0 & v_A^2 \sin \theta \cos \theta \\ 0 & -v_A^2 & 0 \\ c^2 \sin \theta \cos \theta & 0 & -c^2 \sin^2 \theta \end{bmatrix} + \frac{i}{\omega} \begin{bmatrix} \frac{\sigma_P}{\epsilon_\perp} & -\frac{\sigma_H}{\epsilon_\perp} & 0 \\ \frac{\sigma_H}{\epsilon_\perp} & \frac{\sigma_P}{\epsilon_\perp} & 0 \\ 0 & 0 & \frac{\omega_P^2}{\nu - i\omega} \end{bmatrix} \quad (3.6)$$

Nontrivial solutions exist only when $|\underline{\underline{T}}| = 0$. This gives rise to a seventh-order polynomial in ω , so it's necessary to consider limits of particular interest.

3.1 Parallel Propagation Limit

Parallel propagation is a naive representation of a field line resonance; the wave vector moves energy along the field line. Taking $\theta = 0$, $\underline{\underline{T}}$ simplifies to

$$\underline{\underline{T}}_{\parallel} = \underline{\underline{\mathbb{I}}} - \frac{k^2 v_A^2}{\omega^2} \begin{bmatrix} 1 & 0 & 0 \\ 0 & 1 & 0 \\ 0 & 0 & 0 \end{bmatrix} + \frac{i}{\omega} \begin{bmatrix} \frac{\sigma_P}{\epsilon_\perp} & -\frac{\sigma_H}{\epsilon_\perp} & 0 \\ \frac{\sigma_H}{\epsilon_\perp} & \frac{\sigma_P}{\epsilon_\perp} & 0 \\ 0 & 0 & \frac{\omega_P^2}{\nu - i\omega} \end{bmatrix} \quad (3.7)$$

Conveniently, parallel and perpendicular polarizations are not coupled in equation (3.7).

3.1.1 Parallel Polarization

The parallel component of the determinant of equation (3.7) gives

$$\omega^2 + i\nu\omega - \omega_P^2 = 0 \quad (3.8)$$

With no k dependence this expression doesn't describe a wave per se, so much as a resonant frequency. Solving directly,

$$\omega = -\frac{i\nu}{2} \pm \sqrt{\omega_P^2 - \frac{\nu^2}{4}} \quad (3.9)$$

The plasma frequency significantly exceeds the collision frequency everywhere except a narrow strip at the ionospheric boundary of the model. Expanding in large ω_P gives

$$\omega^2 = \omega_P^2 - i\nu\omega_P + \dots \quad (3.10)$$

TODO: Actually, double-check this. How does ν compare to ω_P at the ionospheric boundary when there is no Boris factor?

This is the plasma oscillation.

3.1.2 Perpendicular Polarization

The perpendicular components of the determinant of equation (3.7) give

$$\omega^4 + 2i\frac{\sigma_P}{\epsilon_\perp}\omega^3 - \left(2k^2v_A^2 + \frac{\sigma_P^2 + \sigma_H^2}{\epsilon_\perp^2}\right)\omega^2 - 2ik^2v_A^2\frac{\sigma_P}{\epsilon_\perp}\omega + k^4v_A^4 = 0 \quad (3.11)$$

This can be solved in exact form. Noting that \pm and \oplus are independent,

$$\omega = \left(\frac{\pm\sigma_H - i\sigma_P}{2\epsilon_\perp}\right) \oplus \sqrt{k^2v_A^2 + \left(\frac{\pm\sigma_H - i\sigma_P}{2\epsilon_\perp}\right)^2} \quad (3.12)$$

Over the vast majority of a field line, $kv_A \gg \frac{\sigma_P}{\epsilon_\perp}$ and $kv_A \gg \frac{\sigma_H}{\epsilon_\perp}$.

$$\omega^2 = k^2 v_A^2 \oplus kv_A \frac{\sigma_H \pm i\sigma_P}{\epsilon_\perp} + \dots \quad (3.13)$$

This is the Alfvén wave, evidently split by the ionospheric conductivity, propagating along the zeroth-order magnetic field line.

3.2 Perpendicular Propagation Limit

A wave's ability to propagate across field lines is also of interest. When $\theta = \frac{\pi}{2}$, \underline{T} simplifies to

$$\underline{T}_\perp = \underline{\mathbb{I}} - \frac{k^2}{\omega^2} \begin{bmatrix} 0 & 0 & 0 \\ 0 & v_A^2 & 0 \\ 0 & 0 & c^2 \end{bmatrix} + \frac{i}{\omega} \begin{bmatrix} \frac{\sigma_P}{\epsilon_\perp} & -\frac{\sigma_H}{\epsilon_\perp} & 0 \\ \frac{\sigma_H}{\epsilon_\perp} & \frac{\sigma_P}{\epsilon_\perp} & 0 \\ 0 & 0 & \frac{\omega_P^2}{\nu - i\omega} \end{bmatrix} \quad (3.14)$$

As in the parallel propagation case, the parallel and perpendicular components of the determinant are decoupled.

3.2.1 Parallel Polarization

The parallel component of the determinant of equation (3.14) gives

$$\omega^3 + i\nu\omega^2 - (k^2c^2 + \omega_P^2)\omega - ik^2c^2\nu = 0 \quad (3.15)$$

The above expression can be solved exactly, but the resulting expressions are too long to be useful.

Expanding the solution in large ω_P gives the O mode: a compressional wave with a parallel electric field.

$$\omega^2 = k^2c^2 + \omega_P^2 - i\nu\omega_P + \dots \quad (3.16)$$

3.2.2 Perpendicular Polarization

The perpendicular components of the determinant of equation (3.14) give

$$\omega^3 + 2i\frac{\sigma_P}{\epsilon_\perp}\omega^2 - \left(2k^2v_A^2 + \frac{\sigma_P^2 + \sigma_H^2}{\epsilon_\perp^2}\right)\omega - ik^2v_A^2\frac{\sigma_P}{\epsilon_\perp} = 0 \quad (3.17)$$

Again, the roots of the cubic are impractically long.

Expanding in large conductivity, as is expected near the ionospheric boundary, gives

$$\omega^2 = k^2v_A^2 + \left(\frac{\sigma_H \pm i\sigma_P}{\epsilon_\perp}\right)^2 + \dots \quad (3.18)$$

Whereas expanding in small conductivity, as is expected far from the boundary, gives

$$\omega^2 = k^2v_A^2 \pm ikv_A\frac{\sigma_P}{\epsilon_\perp} + \dots \quad (3.19)$$

Both of which are Alfvén waves.

3.3 High Altitude Limit

At high altitude, where the density is very low compared to the ionosphere, it's reasonable to approximate $\sigma_P \rightarrow 0$ and $\sigma_H \rightarrow 0$ and $\nu \rightarrow 0$.

In this case, \underline{T} simplifies to

$$\underline{T}_\infty = \underline{\mathbb{I}} - \frac{k^2}{\omega^2} \begin{bmatrix} v_A^2 \cos^2 \theta & 0 & -v_A^2 \sin \theta \cos \theta \\ 0 & v_A^2 & 0 \\ -c^2 \sin \theta \cos \theta & 0 & c^2 \sin^2 \theta \end{bmatrix} - \frac{\omega_P^2}{\omega^2} \begin{bmatrix} 0 & 0 & 0 \\ 0 & 0 & 0 \\ 0 & 0 & 1 \end{bmatrix} \quad (3.20)$$

In this case it's the azimuthal polarization that decouples from the other two.

3.3.1 Azimuthal Polarization

The azimuthal component of the determinant of equation (3.20) simply gives the Alfvén wave.

$$\omega^2 = k^2 v_A^2 \quad (3.21)$$

3.3.2 Meridional Polarization

The components of the determinant of equation (3.20) which fall in the meridional plane give, taking $k_\perp \equiv k \sin \theta$ and $k_\parallel \equiv k \cos \theta$,

$$\omega^4 - \left(k_\parallel^2 v_A^2 + k_\perp^2 c^2 + \omega_P^2 \right) \omega^2 + k_\parallel^2 v_A^2 \omega_P^2 = 0 \quad (3.22)$$

The above expression is quadratic in ω^2 , and thus can be solved directly.

$$\omega^2 = \frac{1}{2} \left(k_\parallel^2 v_A^2 + k_\perp^2 c^2 + \omega_P^2 \right) \pm \sqrt{\frac{1}{4} \left(k_\parallel^2 v_A^2 + k_\perp^2 c^2 + \omega_P^2 \right)^2 - k_\parallel^2 v_A^2 \omega_P^2} \quad (3.23)$$

Noting that ω_P is very large, the two roots simplify to

$$\omega^2 = k_\parallel^2 v_A^2 + \dots \quad (3.24)$$

$$\omega^2 = k_\parallel^2 v_A^2 + k_\perp^2 c^2 + \omega_P^2 + \dots \quad (3.25)$$

3.4 Implications for This Work

3.4.1 Mode Coupling

TODO: Have we got enough/appropriate math here to talk about how σ_H rotates fields at the ionosphere? Doubtful.

3.4.2 High Modenumber Cutoff

As m becomes large, it puts a lower bound on the modenumber, and thus on the frequency. For an Alfvén wave, $\omega^2 = k^2 v_A^2$,

$$k \geq k_\phi = \frac{m}{2\pi r} \quad \text{so} \quad \omega \geq \frac{m}{2\pi r} v_A \quad (3.26)$$

Any wave with a frequency below this threshold will become evanescent.

Chapter 4

Numerical Model

The model works in two and a half dimensions. A meridional slice of the magnetosphere is resolved. Fields are presumed to vary azimuthally according to a fixed modenumber m . Derivatives in ϕ are replaced by im . Imaginary field values indicate a phase shift in the azimuthal direction.

TODO: Note that Lysak's 2013 paper[4] was 2.5D.

The use of a fixed modenumber allows a dramatic decrease in computational cost. Waves with very high azimuthal modenumber are prohibitively expensive to simulate since they can only be resolved if grid resolution is very fine in the azimuthal direction.

TODO: Has anyone actually talked about computational expense as a constraint on high- m simulations?

This prevents the simultaneous consideration of dayside and nightside phenomena, but is fine for azimuthally-localized waves. As was shown by [5], and recently confirmed in detail by [2], Pc4 pulsations are generally confined to just a few hours MLT on the dayside.

Driving with a compressional pulse from the outer boundary of a simulation is typical. This model also includes a novel driving mechanism: perturbations to the ring current.

The code is linear. All magnetic fields are a first-order perturbation over the zeroth-order dipole field. This is a not-great assumption out towards the magnetopause. In practice, however, most activity is within $L \sim 7 R_E$, where the dipole approximation is pretty good.

Models with height-resolved ionospheres are a very recent development. Lysak presented his in 2013[4].

Ground signatures are fairly recent as well.

TODO: Some ground signature work as far back as Greifinger and Greifinger in 1968, but there's been steady advancement. Lysak and Song, in 2006, were the first to work out ground signatures without the assumption of a single-frequency wave.

TODO: The support software – the driver and the plotter – are significant too. Do they go in a section? In an appendix?

TODO: Past FLR simulations focused on a single mode, didn't account well for the ionosphere, etc. Lee and Lysak 1989, 1990, 1991, Rankin et al 1993, 1995, 1999, Tikhonchuk and Rankin 2000, 2002.

TODO: Past work that got ground signatures (without latitude-dependent zenith angle) Greifinger and Greifinger 1968, 1973, Hughes 1974, Sciffer and Waters 2002, Sciffer et al 2005. Better computation of ground signatures... Waters and Sciffer 2008, Sciffer and Waters 2011, Woodroffe and Lysak 2012.

Note that the model uses Mm, s, MC, and g as the fundamental units of length, time, charge, and mass respectively. As a result, electric field is measured in mV/m, magnetic field is measured in nT, and Poynting flux is measured in mW/m².

4.1 Coordinate System

When referring to fields in place, it's convenient to use lowercase¹ x , y , and z in their usual dipolar sense. The unit vector \hat{z} is aligned with the dipole field (pointing outward in the northern hemisphere and inward in the southern hemisphere), while \hat{x} is

¹ Not to be confused with uppercase X , Y , and Z , which orient relative to the sun; see chapter 1

perpendicular to \hat{z} within the meridional plane and \hat{y} points in the azimuthal direction.

TODO: Double-check the signs for x (radially inward or outward at the equator?) and y (east or west?).

TODO: Wait... are x , y , and z the same as Radoski's coordinates?

It's convenient to align the grid with the zeroth-order magnetic field, which is presumed to be a perfect dipole. Field line resonances (such as Pc4 pulsations) are guided by magnetic field lines.

TODO: Who showed that ULF waves can be guided? Cite them.

TODO: Discuss, in Future Work, how the grid would be generalized.

Radoski did theoretical work in the following dipole coordinates[6].

$$\mu = -\frac{\sin^2 \theta}{r} \quad \phi = \phi \quad \nu = \frac{\cos \theta}{r^2} \quad (4.1)$$

TODO: The symbol ν is overused. Reserve it for collision frequency. Use something else here.

It's also convenient to take into account the effects of the ionosphere, the lower boundary of which is governed by gravity, and thus has a more-or-less constant altitude. If the above coordinates are used, no line of constant ν coincides with the ionosphere, at least not over a significant range of latitudes.

Many previous works have used an effective ionosphere of nonuniform altitude.

TODO: Figure out which previous works are worth citing here. Options include Radoski 1967, Lee and Lysak 1989, 1991, Rankin et al 1993, 1994, Streltsov and Lotko 1995, 1999.

TODO: "The ionosphere is important for Alfvén waves." Cite this.

In order to accommodate dipole field lines as well as a fixed-altitude ionosphere, a nonorthogonal grid is necessary. Such a grid was worked out numerically by Proehl[7],

then formalized analytically by Lysak[8]:

$$u^1 = -\frac{R_I}{r} \sin^2 \theta \quad u^2 = \phi \quad u^3 = \frac{R_I^2 \cos \theta}{r^2 \cos \theta_0} \quad (4.2)$$

The term R_I indicates the ionosphere's position relative to Earth's center. It's generally taken to be $1 R_E + 100 \text{ km}$.

Like μ and ϕ , the coordinates u^1 and u^2 index a field line. However, compared to ν , u^3 has been renormalized by $\cos \theta_0$, where θ_0 is the colatitude where each field line intersects the ionosphere in the northern hemisphere. As a result, for all field lines, $u^3 = \pm 1$ at the northern and southern foot points.

In terms of the McIlwain parameter, $u^1 = -\frac{R_I}{L}$, and $\cos \theta_0 = \sqrt{1 - \frac{R_I}{L}}$

Compared to equation (4.1), equation (4.2) represents a renormalization of indexing along each field line. The field lines themselves are not deformed.

TODO: Explain how we set up the grid. It should only take a paragraph or two – it doesn't need its own section.

TODO: Plot of the grid setup!

4.1.1 Covariant and Contravariant Bases

The coordinates defined in equation (4.2) are not orthonormal. As a result, it's necessary to consider covariant and contravariant basis vectors separately.

Covariant basis vectors $e_i \equiv \frac{\partial}{\partial u^i} \underline{x}$ are normal to the curve defined by constant u^i .

Contravariant basis vectors $e^i \equiv \frac{\partial}{\partial \underline{x}} u^i$ are tangent to the coordinate curve. Equally, they're normal to the plane defined by constant u^j for all $j \neq i$.

The basis vectors are reciprocal to one another[9], and can be used to define the metric tensor g .

$$\hat{e}^i \cdot \hat{e}_j = \delta_j^i \quad \hat{e}_i \cdot \hat{e}_j = g_{ij} \quad \hat{e}^i \cdot \hat{e}^j = g^{ij} \quad (4.3)$$

Note δ_j^i is the Kronecker delta, ε^{ijk} is the Levi-Civita symbol, and summation is implied over repeated indices per Einstein's convention [10].

The metric tensor is used to map between the covariant and contravariant representations of a vector

$$A_i = g_{ij} A^j \quad A^i = g^{ij} A_j \quad \text{where} \quad A_i \equiv \underline{A} \cdot \hat{e}_i \quad A^i \equiv \underline{A} \cdot \hat{e}^i \quad (4.4)$$

The Jacobian, used for mapping differential volume elements between bases, can be expressed as the square root of the determinant of the metric tensor.

$$G = \sqrt{\varepsilon^{ijk} g_{1i} g_{2j} g_{3k}} \quad \text{where} \quad G du^1 du^2 du^3 = dV \quad (4.5)$$

This quantity is also used when expressing a curl or cross product in generalized coordinates.

$$(\nabla \times \underline{A})^i = \frac{\varepsilon^{ijk}}{G} \frac{\partial}{\partial u^j} A_k \quad (\underline{A} \times \underline{B})^i = \frac{\varepsilon^{ijk}}{G} A_j B_k \quad (4.6)$$

4.1.2 Mapping to Physical Coordinates

The full expression for the basis vectors, metric tensor, and Jacobian determinant discussed in section 4.1.1 can be found in the appendix of [8].

TODO: These expressions should probably be written out in an appendix here too...

The basis vectors can be renormalized to produce unit vectors along the dipole coordinates x , y , and z .

$$\hat{x} = \frac{1}{\sqrt{g^{11}}} \hat{e}^1 \quad \hat{y} = \frac{1}{\sqrt{g^{22}}} \hat{e}^2 \quad \hat{z} = \frac{1}{\sqrt{g^{33}}} \hat{e}^3 \quad (4.7)$$

In addition, this coordinate system provides horizontal and radial unit vectors. Note

that equation (4.8) is valid only at the ionospheric boundary.

$$\hat{\theta} = \frac{1}{\sqrt{g_{11}}} \hat{e}_1 \quad \hat{\phi} = \frac{1}{\sqrt{g_{22}}} \hat{e}_2 \quad \hat{r} = \frac{1}{\sqrt{g_{33}}} \hat{e}_3 \quad (4.8)$$

4.2 Ionospheric Profile

The ionospheric profiles used in this model are based on values tabulated in the Appendix B of Kelley's book[11]. They were adapted by Lysak[4] to take into account the effect of the magnetosphere's latitude-dependent density profile.

Mean molecular mass of 28 u at 100 km, 16 u around 400 km, down to 1 u above 1400 km.

Simulations are carried out using four profiles: active day, quiet day, active night, quiet night.

Profiles are static for the duration of a simulation. Even so-called ultra low frequency waves are still much faster than convective timescales.

TODO: Come up with a characteristic convective timescale or two, and cite it.

4.2.1 Conductivity

The conductivity profiles used in this model are the tabulated values from [11], rescaled by Lysak[4] to account for the increased mean molecular mass at low altitudes.

$$\sigma_P = \sum_s \frac{n_s q_s^2}{m_s} \frac{\nu_s}{\nu_s^2 + \Omega_s^2} \quad \sigma_H = - \sum_s \frac{n_s q_s^2}{m_s} \frac{\Omega_s}{\nu_s^2 + \Omega_s^2} \quad \sigma_0 = \sum_s \frac{n_s q_s^2}{m_s \nu_s} \quad (4.9)$$

Each profile is resolved to an altitude of about 1×10^4 km, and include well-resolved E , F_1 , and F_2 layers.

TODO: Talk about the ionospheric layers, probably in the introduction.

Pedersen (Blue), Hall (Red), and Parallel (Green) Conductivities

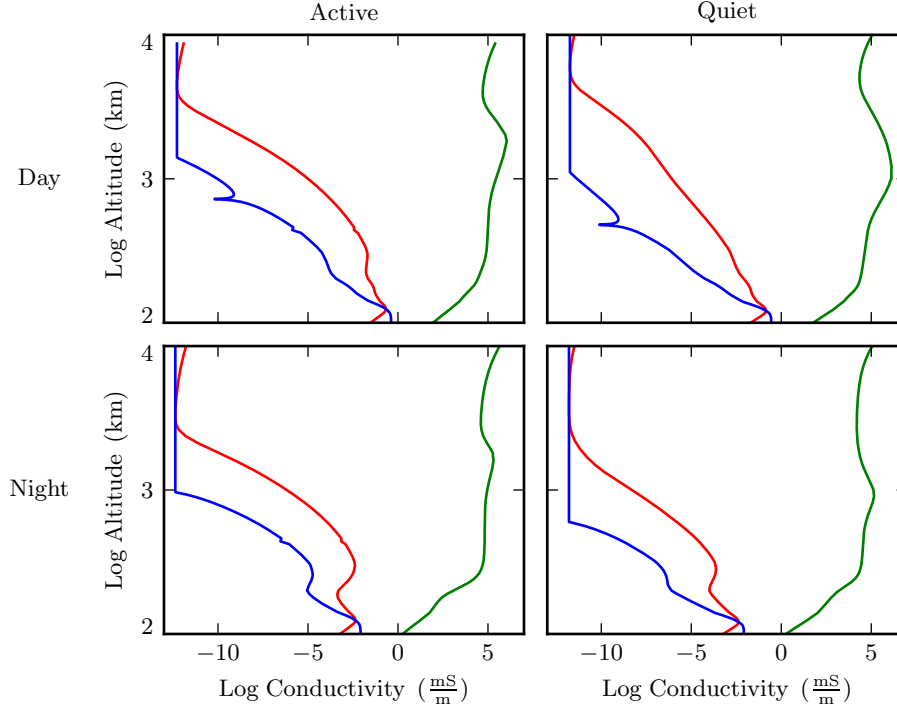


Figure 4.1: Ionospheric conductivity profiles, adapted by Lysak[4] from Appendix B of Kelley's textbook[11].

4.2.2 Alfvén Speed

The Alfvén speed is computed from Kelley's low-density profile, modified to take into account the local density. The density, in turn, is the sum of a plasmaspheric profile and a high-latitude auroral profile.

$$\epsilon_{\perp} = (\text{low-density tabulated value}) + \frac{n\bar{m}}{B_0^2} \quad (4.10)$$

TODO: What's a clean way of showing the low-density ϵ_{\perp} that we read in?

TODO: Above the profile, Bob scales the value that's read in as r^5 or something. Is there a citation for that?

Where \bar{m} is the ambient mean molecular mass and B_0 is the zeroth-order magnetic field strength, $B_0 = 3.11 \times 10^4 \text{ nT} \left(\frac{R_E}{r} \right)^3 \sqrt{1 + 3 \cos^2 \theta}$. Note that $3.11 \times 10^4 \text{ nT}$ is the value of the Earth's magnetic field at the equator on Earth's surface.

TODO: Cite this number?

Note that we do not scale the electric constant to units of ϵ_0 .

The Alfvén speed is then computed per equation (3.5), $v_A^2 \equiv \frac{1}{\mu_0 \epsilon_{\perp}}$.

TODO: Put up a plot of the four Alfvén speed profiles. Show the dipole, or zoom in on the ionosphere?

TODO: Shouldn't the Alfvén speed profiles be brought up early on, since they're necessary for discussions about evanescence at large m in chapter 3?

TODO: Explain in this section how we figure out the time step.

4.3 Maxwell's Equations

The model simulates the evolution of electric and magnetic fields in accordance with Maxwell's equations. Specifically, magnetic fields are advanced using Faraday's Law, and electric fields with Ampère's Law. Kirchhoff's formulation of Ohm's Law ($\underline{J} = \underline{\sigma} \cdot \underline{E}$) is used to eliminate the explicit current dependence in Ampère's Law.

$$\frac{\partial}{\partial t} \underline{B} = -\nabla \times \underline{E} \qquad \underline{\epsilon} \cdot \frac{\partial}{\partial t} \underline{E} = \frac{1}{\mu_0} \nabla \times \underline{B} - \underline{\sigma} \cdot \underline{E} \quad (4.11)$$

4.3.1 Notation and Optimization

Algebra is carried out on paper, producing expressions where each field value is a linear combination of previous field values. These coefficients are computed before the main loop begins. This offers a significant reduction in floating point operations each iteration.

The \leftarrow operator is used to indicate assignment, rather than equality. Values on the left are new, and those on the right are old. New and old magnetic field values are offset by δt ; electric field values staggered by $\frac{\delta t}{2}$. As an example of this notation, equation (4.12) integrates Faraday's Law over a time step, assuming that the curl of the electric field varies slowly compared to δt :

$$\begin{aligned}\int_0^{\delta t} dt \frac{\partial}{\partial t} \underline{B} &= - \int_0^{\delta t} dt \nabla \times \underline{E} \\ \underline{B}|_{\delta t} - \underline{B}|_0 &= -\delta t \nabla \times \underline{E}|_{\frac{\delta t}{2}} \\ \underline{B} &\leftarrow \underline{B} - \delta t \nabla \times \underline{E}\end{aligned}\tag{4.12}$$

It's also beneficial to store the curl of each field, rather than take derivatives on the fly. The following sections make use of the shorthand $\underline{C} \equiv \nabla \times \underline{E}$ and $\underline{F} \equiv \nabla \times \underline{B}$. Or, recalling equation (4.6),

$$C^i = \frac{\varepsilon^{ijk}}{G} \frac{\partial}{\partial u^j} E_k \qquad F^i = \frac{\varepsilon^{ijk}}{G} \frac{\partial}{\partial u^j} B_k \tag{4.13}$$

Only covariant field components are stored. Only contravariant curl components are stored. This cuts down on memory use, while also eliminating the time spent rotating between bases; those operations are built into the precomputed coefficients.

4.3.2 Magnetic Fields

Taking advantage of the shorthand defined in equation (4.13), Faraday's Law is simply written

$$\frac{\partial}{\partial t} B^i = -C^i \tag{4.14}$$

Or, using the metric tensor to cast the magnetic field in terms of its covariant components, and writing out each coefficient explicitly,

$$\begin{aligned} B_1 &\leftarrow B_1 - g_{11} \delta t C^1 - g_{13} \delta t C^3 \\ B_2 &\leftarrow B_2 - g_{22} \delta t C^2 \\ B_3 &\leftarrow B_3 - g_{31} \delta t C^1 - g_{33} \delta t C^3 \end{aligned} \tag{4.15}$$

4.3.3 Electric Fields

Ampère's Law, can be solved with integrating factors. From equation (4.11),

$$\underline{\epsilon} \cdot \frac{\partial}{\partial t} \underline{E} = \frac{1}{\mu_0} \nabla \times \underline{B} - \underline{\sigma} \cdot \underline{E} \tag{4.16}$$

The permittivity tensor is diagonal, and so can be trivially inverted.

$$\left(\underline{\Omega} + \underline{\mathbb{I}} \frac{\partial}{\partial t} \right) \cdot \underline{E} = \underline{v}^2 \cdot \underline{F} \tag{4.17}$$

Where $\underline{\mathbb{I}}$ is the identity tensor and in x - y - z coordinates,

$$\underline{v}^2 \equiv \frac{1}{\mu_0 \underline{\epsilon}} = \begin{bmatrix} v_A^2 & 0 & 0 \\ 0 & v_A^2 & 0 \\ 0 & 0 & c^2 \end{bmatrix} \quad \text{and} \quad \underline{\Omega} \equiv \underline{\epsilon}^{-1} \cdot \underline{\sigma} = \begin{bmatrix} \frac{\sigma_P}{\epsilon_{\perp}} & -\frac{\sigma_H}{\epsilon_{\perp}} & 0 \\ \frac{\sigma_H}{\epsilon_{\perp}} & \frac{\sigma_P}{\epsilon_{\perp}} & 0 \\ 0 & 0 & \frac{\sigma_0}{\epsilon_0} \end{bmatrix} \tag{4.18}$$

Using integrating factors, equation (4.17) gives

$$\underline{E} \leftarrow \exp(-\underline{\Omega} \delta t) \cdot \underline{E} + \delta t \underline{v}^2 \cdot \exp(-\underline{\Omega} \frac{\delta t}{2}) \cdot \underline{F} \tag{4.19}$$

TODO: Do we need to be careful here about the difference between a matrix and a tensor?

The tensor exponential can be evaluated by considering the diagonal and off-diagonal

terms separately.

$$\underline{\underline{\Omega}} = \underline{\underline{\Omega'}} + \frac{\sigma_H}{\epsilon_\perp} \begin{bmatrix} 0 & -1 & 0 \\ 1 & 0 & 0 \\ 0 & 0 & 0 \end{bmatrix} \quad \text{where} \quad \underline{\underline{\Omega'}} = \begin{bmatrix} \frac{\sigma_P}{\epsilon_\perp} & 0 & 0 \\ 0 & \frac{\sigma_P}{\epsilon_\perp} & 0 \\ 0 & 0 & \frac{\sigma_0}{\epsilon_0} \end{bmatrix} \quad (4.20)$$

Note that tensors are remarkably well-behaved when exponentiated[12], particularly since $\underline{\underline{\Omega'}}$ is diagonal, and thus they commute.

$$\exp(\underline{\underline{T}}) = \sum_n \frac{1}{n!} \underline{\underline{T}}^n \quad \text{and} \quad \exp(\underline{\underline{T}} + \underline{\underline{T'}}) = \exp(\underline{\underline{T}}) \exp(\underline{\underline{T'}}) \quad (4.21)$$

The off-diagonal terms collapse into sines and cosines, indicating a rotation about z .

$$\underline{E} \leftarrow \exp(-\underline{\underline{\Omega'}} \delta t) \cdot \underline{\underline{R}}_z \left(\frac{-\sigma_H \delta t}{\epsilon_\perp} \right) \cdot \underline{E} + \delta t \underline{v}^2 \cdot \exp(-\underline{\underline{\Omega'}} \frac{\delta t}{2}) \cdot \underline{\underline{R}}_z \left(\frac{-\sigma_H \delta t}{2\epsilon_\perp} \right) \cdot \underline{F} \quad (4.22)$$

Where

$$\underline{\underline{R}}_z(\theta) = \begin{bmatrix} \cos \theta & -\sin \theta & 0 \\ \sin \theta & \cos \theta & 0 \\ 0 & 0 & 1 \end{bmatrix} \quad (4.23)$$

The parallel term of term of equation (4.22) is simply

$$E_\parallel \leftarrow E_\parallel \exp\left(\frac{-\sigma_0 \delta t}{\epsilon_0}\right) + c^2 \delta t F_\parallel \exp\left(\frac{-\sigma_0 \delta t}{2\epsilon_0}\right) \quad (4.24)$$

For the aforementioned ionospheric profiles and time steps, $\frac{\sigma_0 \delta t}{\epsilon_0}$ is never smaller than 10^3 . As a result, $\exp\left(-\frac{\sigma_0 \delta t}{\epsilon_0}\right)$ is far too small to be stored in a double precision variable. That is, this simulation takes E_\parallel (and, equally, E_3) to be uniformly zero.

This, obviously, precludes any discussion of parallel electric fields or parallel currents. These topics are revisited in chapter 5.

Not unrelatedly, recalling the definition of the plasma frequency and parallel conductivity from equation (3.5), $\frac{\sigma_0}{\epsilon_0}$ can also be written $\frac{\omega_P^2}{\nu}$.

The plasma frequency is very fast.

The perpendicular components of equation (4.22), mapped from the physical basis to the contravariant basis (per equation (4.7)) to the covariant basis (per equation (4.4)), give

$$\begin{aligned}
E_1 + \frac{g^{13}}{g^{11}}E_3 \leftarrow & E_1 \cos\left(\frac{-\sigma_H \delta t}{\epsilon_\perp}\right) \exp\left(\frac{-\sigma_P \delta t}{\epsilon_\perp}\right) \\
& + E_2 \sin\left(\frac{-\sigma_H \delta t}{\epsilon_\perp}\right) \exp\left(\frac{-\sigma_P \delta t}{\epsilon_\perp}\right) \sqrt{\frac{g^{22}}{g^{11}}} \\
& + E_3 \cos\left(\frac{-\sigma_H \delta t}{\epsilon_\perp}\right) \exp\left(\frac{-\sigma_P \delta t}{\epsilon_\perp}\right) \frac{g^{13}}{g^{11}} \\
& + F^1 \cos\left(\frac{-\sigma_H \delta t}{2\epsilon_\perp}\right) \exp\left(\frac{-\sigma_P \delta t}{2\epsilon_\perp}\right) \frac{v_A^2 \delta t}{g^{11}} \\
& + F^2 \sin\left(\frac{-\sigma_H \delta t}{2\epsilon_\perp}\right) \exp\left(\frac{-\sigma_P \delta t}{2\epsilon_\perp}\right) \frac{v_A^2 \delta t}{\sqrt{g^{11}g^{22}}}
\end{aligned} \tag{4.25}$$

and

$$\begin{aligned}
E_2 \leftarrow & -E_1 \sin\left(\frac{-\sigma_H \delta t}{\epsilon_\perp}\right) \exp\left(\frac{-\sigma_P \delta t}{\epsilon_\perp}\right) \sqrt{\frac{g^{11}}{g^{22}}} \\
& + E_2 \cos\left(\frac{-\sigma_H \delta t}{\epsilon_\perp}\right) \exp\left(\frac{-\sigma_P \delta t}{\epsilon_\perp}\right) \\
& - E_3 \sin\left(\frac{-\sigma_H \delta t}{\epsilon_\perp}\right) \exp\left(\frac{-\sigma_P \delta t}{\epsilon_\perp}\right) \frac{g^{13}}{\sqrt{g^{11}g^{22}}} \\
& - F^1 \sin\left(\frac{-\sigma_H \delta t}{2\epsilon_\perp}\right) \exp\left(\frac{-\sigma_P \delta t}{2\epsilon_\perp}\right) \frac{v_A^2 \delta t}{\sqrt{g^{11}g^{22}}} \\
& + F^2 \cos\left(\frac{-\sigma_H \delta t}{2\epsilon_\perp}\right) \exp\left(\frac{-\sigma_P \delta t}{2\epsilon_\perp}\right) \frac{v_A^2 \delta t}{g^{22}}
\end{aligned} \tag{4.26}$$

The E_3 terms can be ignored at present, but chapter 5 references back to them.

4.4 Driving

If no energy is added, the simulation is pretty boring. Everything just stays zero.

4.4.1 Outer Boundary Compression

Driving from the outer boundary is the traditional way to do it.

TODO: Cite and briefly explain past work done with compressional driving. This is what most of Bob's papers are, right?

As discussed in section 3.4, Alfvén waves become guided when the azimuthal modenum-
ber is large. The energy all stays close to the outer boundary. No field line resonances
of significant strength are created within the magnetosphere.

TODO: Show a plot of compressional driving, maybe day and night, as m increases.
Mean energy density over time? Something that shows the recession of waves away from
the middle of the simulation.

Compressional driving is applied by setting the value of B_3 at the outer boundary.

4.4.2 Ring Current Modulation

Pc4 pulsations with high azimuthal modenum-
ber are known to be driven from within
the magnetosphere, such as through drift-resonant interactions with energetic radiation
belt and ring current particles.

TODO: Cite.

Substorm injection can cause localized ring current behavior.

TODO: UNH was looking at this at AGU. Check if they have published yet.

During geomagnetically active times, the ring current is a dynamic region. It's easy to
imagine localized perturbations.

It's difficult to estimate how large such perturbations might be. The following is a
kludgy estimate.

TODO: Plot of Sym-H and its Fourier modes.

The noise suggests that a Fourier component with a period of about 1 min could have
an amplitude around 10^{-3} nT.

If the driving is delivered at $L = 5$, with a standard deviation of $0.5 R_E$ in the radial direction and 5° angularly, that corresponds to a current density of about $4 \times 10^{-4} \mu\text{A}/\text{m}^2$.

TODO: What electric field magnitude does this correspond to?

Current driving is applied by adding an additional current term. Ampère’s Law becomes

$$\underline{\epsilon} \cdot \frac{\partial}{\partial t} \underline{E} = \frac{1}{\mu_0} \nabla \times \underline{B} - \underline{\sigma} \cdot \underline{E} - \underline{J}_{drive} \quad (4.27)$$

And this driving term is absorbed into the curl by revising equation (4.13) from $\underline{F} \equiv \nabla \times \underline{B}$ to $\underline{F} \equiv \nabla \times \underline{B} - \underline{J}_{drive}$. (As a result, equations (4.25) and (4.26) do not change.)

...

...

...

We look at Sym-H to get an idea of the appropriate scale for current driving. We look at a few storms. 1 June 2013. 17 March 2015. 22 June 2015. 17 March 2013. A few in October and November 2012.

We plot the power spectrum and basically do a fit for the top of the range of $\frac{1}{f}$ noise. This gives us a typical magnitude for oscillations on the order of a minute.

This doesn’t give us a characteristic spatial extent for ring current modulations – Sym-H is a global index – but we can eyeball the size of current fluctuations. We know the approximate size of the ring current, so we can go from ground-based field signature to current density in space pretty easily.

There are a lot of parameters to play with. Since this is a linear code, we don’t have to worry about “sweet spots” for nonlinear effects in the driving magnitude. And it doesn’t look like the exact position or shape of the ring current has much qualitative effect on what we see.

Looking at SYMH. Fourier series out to a period of about a minute. The power spectrum (judging from June 1-3 2013) gives you $10^{-2}(T/minutes)$. We can hand-wave a mapping from SYMH to the ring current.

$$B = \frac{\mu_0 I}{2R} \quad (4.28)$$

With $B \sim 2 \text{ nT}$, $R \sim 4 R_E$, $A \sim 1 R_E \sigma_P 2$, we end up with $J \sim 10^{-4} \mu\text{A}/\text{m}^2$.

4.5 Boundary Conditions

The grid can't go on forever. There have to be special cases at the edges.

4.5.1 Parity and Interpolation

At the inner and outer boundaries (that is, along the innermost and outermost field lines), as use Dirichlet and Neumann boundary conditions for electric and magnetic fields respectively.

These are implemented in the differentiation and (parity) interpolation functions.

Whenever we need to know the magnetic field just outside the grid boundary, we say that its value is the same as just inside the grid boundary, and its derivative is zero. Neumann.

Conversely, we say that the electric field just outside the grid goes to 0, allowing us to compute the derivative from the value just inside the grid. Dirichlet.

Dirichlet and Neumann could be flipped without much consequence. They're sorta arbitrary. But mixing up a term, so that they are no longer self-consistent, causes instability.

Each field component is stored at only one parity in each direction. This is because of how curls line up. Adjacent values of E_2 just aren't really coupled to each other.

This means that computing all of the parities isn't just unnecessary – it's potentially unstable. The odd-by-odd grid and the odd-by-even grid are only weakly coupled, especially at large r , so they can drift apart. This can lead to problems in places where they do care about one another. This is documented... where???

This would be perfectly true if we were taking curls on an orthonormal grid, and if there was no Hall conductivity. As is, it's still pretty true. The contributions of off-parity terms tend to be small.

TODO: Bob notes, in talking about forward/backward differences at the boundary, that the boundary can cause nonphysical reflections, but that they are in practice not relevant to the results.

4.5.2 Coupling to the Atmosphere

Per Maxwell's equations, $\nabla \cdot \underline{B} = 0$. We further assume that there are no currents flowing in the atmosphere, giving $\nabla \times \underline{B} = 0$. These conditions together guarantee the existence of a scalar magnetic potential, Ψ , which satisfies Laplace's equation, $\nabla^2 \Psi = 0$ and $\underline{B} = \nabla \Psi$.

Separating out the r and ϕ components of Laplace's equation, the θ component of the equation can be written as a differential equation in terms of $u \equiv \cos \theta$:

$$\frac{d}{du} \left((1 - u^2) \frac{d}{du} Y_\nu \right) - \frac{m^2}{1 - u^2} Y_\nu = -\nu(\nu + 1) Y_\nu \quad (4.29)$$

This can be solved numerically on our discrete grid, providing us with eigenvectors and eigenvalues (Y_ν and ν respectively). We can then write Ψ in terms of those harmonics:

$$\Psi(r, \theta) = \sum_{\nu} (\alpha_{\nu} r^{\nu} + \beta_{\nu} r^{-\nu-1}) Y_{\nu}(\theta) \quad (4.30)$$

We will rearrange this expression in order to compute Ψ each time step as a linear combination of the radial magnetic field values at R_I .

We defined $\underline{B} = \nabla \Psi$, so $B_r = \frac{\partial}{\partial r} \Psi$.

The ground is perfectly conducting, so $B_r(R_E) = 0$.

...

We don't need to show algebra, but we should show the final expression.

...

Jump condition over the ionospheric current sheet. This comes from integrating Ampère's Law... ?

TODO: Bob's citations for the ionospheric jump conditions: Fujita and Tamao 1988, Yosikawa and Itonaga 1996, 2000, Lysak and Song 2001, Sciffer and Waters 2002.

Chapter 5

Electron Inertial Effects

TODO: Bob mentions something about electron inertia or pressure being in his 2011 paper.

COPIED OVER FROM THE MODEL CHAPTER.

Parallel Ampère's Law.

$$\epsilon_{\parallel} \frac{\partial}{\partial t} E_{\parallel} = \frac{1}{\mu_0} (\nabla \times \underline{B})_{\parallel} - J_{\parallel} \quad (5.1)$$

If we follow the same approach as above, we can also solve with integrating factors. There isn't even any rotation.

$$E_{\parallel}(\delta t) = E_{\parallel}(0) \exp\left(-\frac{\sigma_0}{\epsilon_{\parallel}} \delta t\right) + v_A^2 \delta t F_{\parallel}\left(\frac{\delta t}{2}\right) \exp\left(-\frac{\sigma_0}{\epsilon_{\parallel}} \frac{\delta t}{2}\right) \quad (5.2)$$

However, it turns out that the field-aligned conductivity is really big, and the parallel electric constant (assumed to be ϵ_0) is pretty small. For each profile, we see $\frac{\sigma_0}{\epsilon_{\parallel}} \delta t \gtrsim 10^3$. When the exponential is evaluated, it goes to zero.

So, the above expression can't be used to compute parallel electric fields.

We get around that by adding electron inertial effects to Ohm's Law. Recall that in

generalized form, Ohm's Law is:

$$\underline{E} + \underline{U} \times \underline{B} = \eta \underline{J} + \frac{m_e}{ne^2} \left[\frac{\partial}{\partial t} \underline{J} + \nabla \cdot \left(\underline{J} \underline{U} + \underline{U} \underline{J} + \frac{1}{ne} \underline{J} \underline{J} \right) \right] + \frac{1}{ne} \underline{J} \times \underline{B} - \frac{1}{ne} \nabla \cdot \underline{\underline{P_e}} \quad (5.3)$$

We are using a cold, static plasma, so we get to ignore any terms with \underline{U} . We also skip the nonlinear terms... this can probably be justified through a scaling argument.

The parallel conductivity is much larger than the Pedersen and Hall conductivities, which is how we can justify keeping only the parallel component of this term.

After pulling the conductivity tensor out of the denominator, we are left with the same form as before, but with an added term representing electron inertia:

$$\frac{\partial}{\partial t} J_{\parallel} = \frac{ne^2}{m_e} E_{\parallel} - \frac{ne^2}{m_e \sigma_0} J_{\parallel} \quad (5.4)$$

NOTE: MAYBE WE WANT TO WRITE THIS IN TERMS OF THE COLLISION RATE?

Now we solve for J_{\parallel} using integrating factors.

$$J_{\parallel}(\delta t) = J_{\parallel}(0) \exp\left(-\frac{ne^2}{m_e \sigma_0} \delta t\right) + \frac{ne^2}{m_e} \delta t E_{\parallel}\left(\frac{\delta t}{2}\right) \exp\left(-\frac{ne^2}{m_e \sigma_0} \frac{\delta t}{2}\right) \quad (5.5)$$

Or, in covariant terms,

$$J_3(\delta t) = J_3(0) \exp\left(-\frac{ne^2}{m_e \sigma_0} \delta t\right) + E_3\left(\frac{\delta t}{2}\right) \frac{ne^2}{m_e} \delta t \exp\left(-\frac{ne^2}{m_e \sigma_0} \frac{\delta t}{2}\right) \quad (5.6)$$

We see the half-step offset again. The current lines up with the magnetic field.

NOTE: WE HAVE A SYMBOL NOW FOR THE BORIS PLASMA FREQUENCY.

The electron inertial term of Ohm's Law describes plasma oscillation, which (naturally) happen at the plasma frequency. We expect this to be unstable unless $\delta t < \frac{1}{\omega_{pe}}$. We're

off, by a lot.

Reducing the time step by several orders of magnitude is not feasible. Much of what makes this model valuable is its speed – the ability to conduct an ensemble of dozens of runs overnight – and that would be lost if runs went from an hour to four days. This also risks instabilities of its own due to compounding numerical noise.

The solution is to implement a Boris correction, as introduced in (CITE BORIS 1970!!!). We increase ϵ_{\parallel} above its previous value of ϵ_0 . This essentially drops the speed of light and the plasma frequency – potentially by several orders of magnitude – while leaving their ratio, the electron inertial length, unchanged. This can easily reduce the speed of light to less than the Alfvén speed!

This is safe as long as we keep the plasma frequency well above Pc4 frequencies. This was shown in Lysak 2001 (CITE!!!). Also in Ronnmark (CITE!!!), who uses the nice term "anisotropic vacuum".

To briefly summarize Lysak's argument for why this is safe, start with the same equations as above. And assume that we're oscillating at some frequency ω . Then we can evaluate the time derivatives in Ampère's Law and Ohm's Law. Note that we bring in the electron-ion collision frequency $\nu = \frac{ne^2}{m_e \sigma_0}$

$$\epsilon_{\parallel} \frac{\partial}{\partial t} E_{\parallel} = \frac{1}{\mu_0} (\nabla \times \underline{B})_{\parallel} - J_{\parallel} \qquad \frac{\partial}{\partial t} J_{\parallel} = \frac{ne^2}{m_e} E_{\parallel} - \nu J_{\parallel} \qquad (5.7)$$

So with the electron inertial length defined per $\lambda^2 \equiv \frac{c^2}{\omega_p^2} = \frac{m_e}{ne^2 \mu_0} \dots$

$$\left[1 - \frac{\omega^2 - i\omega\nu}{\omega_p^2} \right] E_{\parallel} = \lambda^2 (\nu - i\omega) (\nabla \times \underline{B})_{\parallel} \qquad (5.8)$$

That is, as long as $\frac{\omega}{\omega_p} \ll 1$ and $\frac{\omega\nu}{\omega_p^2} \ll 1$ we should see no difference in the relative scales of the electric and magnetic fields.

Notably, without the electron inertial term, the perpendicular expression has no $i\omega$ on

the right hand side of the expression. That's probably fine. The (effective?) perpendicular collision frequency is very large. (It can't be a real collision frequency... it goes to infinity when number density gets tiny! Note that the different conductivities actually have quite different expressions when derived from first principles.)

... rehashing the above a bit ...

Start with parallel Ampère's Law and Ohm's Law, with electron inertia.

$$\epsilon_{\parallel} \frac{\partial}{\partial t} E_{\parallel} = \frac{1}{\mu_0} (\nabla \times \underline{B})_{\parallel} - J_{\parallel} \qquad \frac{\partial}{\partial t} J = \frac{ne^2}{m} E_{\parallel} - \nu J_{\parallel} \quad (5.9)$$

Assume oscillation as $\exp(-i\omega t)$, evaluate time derivatives, and eliminate J .

$$\left[1 - \frac{\omega^2 + i\omega\nu}{\omega_{\parallel}^2} \right] E_{\parallel} = \lambda^2 (\nu - i\omega) (\nabla \times \underline{B})_{\parallel} \quad (5.10)$$

Where λ , the electron inertial length, and ω_B , the potentially-Boris-adjusted plasma frequency, are given by:

$$\lambda^2 \equiv \frac{c^2}{\omega_p^2} = \frac{m}{ne^2\mu_0} \qquad \omega_B^2 \equiv \frac{ne^2}{m\epsilon_B} \quad (5.11)$$

If parallel currents are included in the model, the time step must satisfy $\omega_{\parallel}\delta t < 1$ for stability. This is a significant constraint. The time step computed from the Alfvén speed and grid geometry is typically on the order of 10 μ s; plasma timescale can be as small as 10 ns. Decreasing the time step by three orders of magnitude means turning a one-hour run into a six-week run.

The plasma timescales can be reduced by introducing a Boris factor; that is, by increasing the electric constant ϵ_{\parallel} above its usual value of ϵ_0 . This serves to reduce the speed of light and plasma frequency without affecting the electron inertial length.

The Boris factor is constrained by the ratio between E_{\parallel} and $(\nabla \times \underline{B})_{\parallel}$ defined in equation (5.10). Any change in $\left[1 - \frac{\omega^2 + i\omega\nu}{\omega_B^2} \right]$ would be expected to significantly affect model behavior.

As shown in (PLOT THE FREQUENCY RATIOS!!!), there's room for a Boris factor of significant size. Even at a factor of 10^6 , $\left| \frac{\omega^2 + i\omega\nu}{\omega_B^2} \right| \lesssim 0.01$.

5.1 The Boris Approximation

5.2 Field-Aligned Currents

5.3 Inertial Length Scales

Chapter 6

Large Modenumber Effects

This is why we do 2.5D... you can't resolve these effects in a 3D model. It's too expensive.

TODO: Do we see a difference between \underline{k} (momentum) and the group velocity? Poynting flux will always be pretty much along the field line, since B_3 is small and E_3 is zero, but the wave vector need not be. This is a question of coupling/converting to compressional waves, I guess.

TODO: Look at McKenzie and Westphal. Waves incident on the bow shock, etc, at weird angles.

TODO: Look at the E to B ratio. Compare to the Alfvén speed and to the height-integrated Pedersen conductivity.

6.1 Finite Poloidal Lifetimes

CITE RADOSKI 1974

CITE MANN 1995

CITE DING 1995

TODO: Look at Mann's poloidal lifetime, $\frac{\partial}{\partial \omega'_A} \lambda$ where $\lambda \sim \frac{m}{2\pi r}$.

6.2 Development of Fine Structure

6.3 Damping of Ground Signatures

6.4 Electromagnetic Energy Gap

Chapter 7

Evolution of Giant Pulsations

Chapter 8

Comparison to Van Allen Probe Observations

TODO: Note that RBSP's ability to measure poloidal/toroidal waves depends on geometry. It always has to guess for one electric field component.

Chapter 9

Conclusion and Discussion

9.1 Future Work

Non-sinusoidal driving, obviously.

Arbitrary deformation of grid. Get $\hat{e}_i = \frac{\partial}{\partial u^i} \underline{x}$, then $g_{ij} = \hat{e}_i \cdot \hat{e}_j$, then invert.

3D using MPI.

References

- [1] Lei Dai, Kazue Takahashi, John R. Wygant, Liu Chen, John Bonnell, Cynthia A. Cattell, Scott Thaller, Craig Kletzing, Charles W. Smith, Robert J. MacDowall, Daniel N. Baker, J. Bernard Blake, Joseph Fennell, Seth Claudepierre, Herbert O. Funsten, Geoffrey D. Reeves, and Harlan E. Spence. Excitation of poloidal standing alfvén waves through drift resonance wave-particle interaction. *Geophys. Res. Lett.*, 40:41274132, 2013.
- [2] Lei Dai, Kazue Takahashi, Robert Lysak, Chi Wang, John R. Wygant, Craig Kletzing, John Bonnell, Cynthia A. Cattell, Charles W. Smith, Robert J. MacDowall, Scott Thaller, Aaron Breneman, Xiangwei Tang, Xin Tao, and Lunjin Chen. Storm time occurrence and spatial distribution of pc4 poloidal ulf waves in the inner magnetosphere: A van allen probes statistical study. *J. Geophys. Res. Space Physics*, 120:47484762, 2015.
- [3] Robert L. Lysak and Yan Song. A three-dimensional model of the propagation of alfvén waves through the auroral ionosphere: first results. *Adv. Space Res.*, 28:813–822, 2001.
- [4] Robert L. Lysak, Colin L. Waters, and Murray D. Sciffer. Modeling of the ionospheric alfvén resonator in dipolar geometry. *J. Geophys. Res. Space Physics*, 118, 2013.
- [5] M. J. Engebretson, L. J. Zanetti, T. A. Potemra, W. Baumjohann, H. L. uhr, and M. H. Acuna. Simultaneous observation of pc 34 pulsations in the solar wind and

- in the earth's magnetosphere. *J. Geophys. Res. Space Physics*, 92:10053–10062, 1987.
- [6] Henry R. Radoski. A note on oscillating field lines. *J. Geophys. Res.*, 72(1), 1967.
 - [7] Jeffrey A. Proehl, William Lotko, Igor Kouznetsov, and Shireen D. Geimer. Ultralow-frequency magnetohydrodynamics in boundary-constrained geomagnetic flux coordinates. *J. Geophys. Res.*, 107(A9):1225, 2002.
 - [8] Robert L. Lysak. Magnetosphere-ionosphere coupling by alfvén waves at midlatitudes. *J. Geophys. Res.*, 109, 2004.
 - [9] W. D. D'haeseleer, W. N. G. Hitchon J. D. Callen, and J. L. Shohet. *Flux Coordinates and Magnetic Field Structure*. Springer-Verlag, New York, 1991.
 - [10] A. Einstein. Die grundlage der allgemeinen relativit atstheorie. *Ann. Phys.*, 354:769–822, 1916.
 - [11] Michael C. Kelley. *The Earth's Ionosphere*. Academic Press, San Diego, second edition, 1989.
 - [12] Brian C. Hall. *Lie Groups, Lie Algebras, and Representations*. Graduate Texts in Mathematics. Springer, New York, second edition, 2015.

Appendix A

Differential Geometry

Care has been taken in this thesis to minimize the use of jargon and acronyms, but this cannot always be achieved. This appendix defines jargon terms in a glossary, and contains a table of acronyms and their meaning.

A.1 Glossary

- **Cosmic-Ray Muon (CR μ)** – A muon coming from the abundant energetic particles originating outside of the Earth’s atmosphere.

A.2 Acronyms

Table A.1: Acronyms

Acronym	Meaning
CR μ	Cosmic-Ray Muon

Appendix B

Integrating Factors

Start with differential equation of the form:

$$\frac{\partial}{\partial t}X(t) + \alpha X(t) = \beta \quad (\text{B.1})$$

Multiply by the integrating factor, then group terms:

$$\exp(\alpha t) \frac{\partial}{\partial t}X(t) + \alpha \exp(\alpha t)X(t) = \beta \exp(\alpha t) \quad (\text{B.2})$$

$$\frac{\partial}{\partial t} [\exp(\alpha t)X(t)] = \beta \exp(\alpha t) \quad (\text{B.3})$$

Integrate from 0 to δt , assuming that β is constant in time or varies slowly.

$$\int_0^{\delta t} dt \frac{\partial}{\partial t} [\exp(\alpha t)X(t)] = \int_0^{\delta t} dt \beta \exp(\alpha t) \quad (\text{B.4})$$

$$\exp(\alpha \delta t)X(\delta t) - X(0) = \delta t \beta \left(\frac{\delta t}{2}\right) \exp\left(\alpha \frac{\delta t}{2}\right) \quad (\text{B.5})$$

Then rearrange to solve for the new value of X:

$$X(\delta t) = X(0) \exp(-\alpha \delta t) + \delta t \beta \left(\frac{\delta t}{2}\right) \exp(-\alpha \frac{\delta t}{2}) \quad (\text{B.6})$$

Done.